Long-term adjustment of the South America Atlantic Forest to atmospheric carbon dioxide concentration

Thiago Santos, Ioanna Bouloubassi, Joana Cruz, Alice Rodrigues, Marie-Pierre Ledru, Arnaud Huguet, Marília Shimizu, Murílo Lemes, Rodrigo Nascimento, Igor Venancio, et al.

Long-term adjustment of the South America Atlantic Forest to atmospheric carbon dioxide concentration

Thiago Santos

thiagopds@usp.br

University of São Paulo https://orcid.org/0000-0002-9273-3329

Ioanna Bouloubassi

Sorbonne Université

Joana Cruz

Fluminense Federal University

Alice Rodrigues

Fluminense Federal University

Marie-Pierre Ledru

Univ Montpellier

Arnaud Huguet

Sorbonne Université

Marília Shimizu

National Institute for Space Research https://orcid.org/0000-0003-0895-555X

Murílo Lemes

National Institute for Space Research

Rodrigo Nascimento

Université Paris Saclay

Igor Venancio

Fluminense Federal University

Rodrigo Sobrinho

Fluminense Federal University

Marcelo Bernardes

Fluminense Federal University

Ana Albuquerque

Universidade Federal Fluminense https://orcid.org/0000-0003-1267-6190

Article

Keywords:

Posted Date: May 9th, 2024

DOI: https://doi.org/10.21203/rs.3.rs-4294907/v1

Additional Declarations: There is **NO** Competing Interest.

Abstract

The effect of CO2 fertilization on tropical forests is uncertain due to a lack of direct data and confounding effects of climate variability. Long-term proxy records could help understand the impact of elevated CO2 on tropical vegetation. We provide observationally inferred evidence that the evolution of the Atlantic Forest in SE Brazil between ~ 150 and 65 ka was influenced by CO2 variability rather than temperature or precipitation on both precessional and millennial time scales. Plant wax n-alkanes in a marine core were used to trace forest cover fluctuations and compared with continental records of fossil pollen, revealing a strong correlation with CO2 levels. This highlights CO2 fertilization as a key driver of the past Atlantic Forest evolution, emphasizing the need for protection initiatives to preserve its long-term capacity in carbon storage. Further research is needed to understand the long-term effects of CO2 on tropical forests at the ecosystem scale.

Introduction

The Neotropical Atlantic Forest is one of the world's most biodiverse and endangered ecosystems[1,2] that originally covered 12 % of Brazil's national territory with a latitudinal range of *ca.* 29° extending into tropical and subtropical regions (Figure 1). The massive agricultural expansion with the arrival of European colonists in the 16th century, followed by intense industrialization and urban development, has resulted in an impressive habitat loss. Currently, the Atlantic Forest is confined to only *ca*. 7 % of its original extent[3] and composed of small, isolated, and degraded fragments, making this ecosystem a global priority for biodiversity conservation[2–4].

Tropical forests, like the Atlantic Forest, are characterized by the dominance of tree life forms, creating a closed canopy and complex arrangements that provide diverse ecosystem services[5]. Among these, carbon uptake is the most recognized, with about one-third of anthropogenic carbon dioxide emitted being removed by such forests[6]. Carbon uptake in terrestrial ecosystems seems to have increased globally[7], likely due to the fertilization effect of rising CO_2 levels. Indeed, one of the primary expected effects of higher atmospheric CO_2 is an increase in the photosynthetic rate and a decrease in the transpiration rate occurring at the enzymatic and stomatal scales, which ultimately regulates C uptake[8–10]. This effect may result in important negative feedback on anthropogenic-induced global warming[11,12]. Otherwise, studies argue that this capacity is not being sustained because increasing air temperature and reduced water availability would raise plant respiration exponentially, reducing forest productivity[13,14]. Such conflicting conclusions emphasize our poor understanding of the long-term response of tropical forests to rising CO_2 levels.

In this regard, paleoclimate data may provide relevant insight for investigating past vegetation changes under naturally varying atmospheric CO_2 concentrations at different time scales. Leaf gas-exchange modeling on temperate and tropical fossil flora from the early Miocene suggests enhanced leaf-level productivity and water-use efficiency under elevated CO_2 (~ 450-550 ppm), which likely contributed to

forest survival in climates where currently tropical savannas and grasslands dominate[15]. In the Quaternary, the triple isotopic ratio of atmospheric oxygen recovered from Antarctica ice cores indicates that marine and terrestrial biosphere productivity changes coeval to glacial-interglacial variability, with the latter largely driven by atmospheric CO_2[16]. In subtropical SE Africa, the main extension of woodlands during the Pleistocene occurred under interglacial conditions of raised CO_2 even though these intervals were regionally drier than glacial periods[17]. Likewise, the Pleistocene evolution of NW African savanna ecosystems was strongly controlled by atmospheric *p*CO2, whereby rising atmospheric carbon dioxide led to increased woody cover[18]. Tropical forests in South America experienced a marked expansion since the Last Glacial Maximum (LGM), leading to a 20%-100% increase in carbon storage[19]. For the Atlantic forest realm, the increase in carbon storage was estimated in the order of 4.9 10^9 tC (55%), making this biome an important locus for atmospheric CO_2 sequestration[19]. Changes in past vegetation cover/dynamics of the Atlantic forest have usually been ascribed to climate (i.e., temperature and moisture), while the (possible) control of atmospheric CO_2 has not been strongly explored[20,21].

Here, we investigate an 85 kyr time interval from late Marine Isotope Stage (MIS) 6 to early MIS 4, which spans over glacial, transitional, and interglacial climate phases, encompassing a large range of CO_2 conditions (from ~ 200 to ~280 ppm)[22,23] and includes periods of different monsoonal rainfall regimes in the South America[24,25]. We provide a record of vegetation changes from plant wax composition and soil-derived discharges based on the abundance of branched glycerol dialkyl glycerol tetraether in a marine sediment core from the continental slope of SE Brazil (GL-1090, 24.92 ºS, 42.51 ºW, 2225 m water depth)[26,27]. The core site receives terrestrial inputs through runoff from the adjacent hinterland that hosts the central and south areas of the South American Atlantic Forest[28]. We discuss our records with regional pollen data, monsoonal precipitation, and global CO_2 concentrations.

Our findings sustain that under natural climate variability, the atmospheric CO_2 concentration is the key driver of the Atlantic Forest changes (arboreal cover) on precessional and millennial time scales. A potential vegetation simulation with the CPTEC-PVM2 model[29] corroborates this interpretation. Our data support the effect of CO_2 fertilization over the Atlantic Forest and urge protection and reforestation initiatives to preserve its natural long-term capacity in carbon storage.

Results

A suite of long chain odd-carbon numbered homologs dominates the distribution of *n*-alkanes and is typical of inputs from epicuticular waxes of terrestrial higher plants[32]. Their Average Chain Length (ACL) varies between 29.6 and 30.7 and exhibits glacial-interglacial oscillations (Figure 2a), with generally higher values during full glacial or cold MIS 5 substages (MIS 5d and 5b). The largest ACL change (~ 0.7) occurs at the transition from the penultimate glacial maximum (late MIS 6) to the Last Interglacial (MIS 5e), where relatively steady low ACL values (~ 29.7) dominate the pattern. From early

MIS 5e toward MIS 4, a Mann-Kendall statistically significant increasing trend exists ($p < 0.01$), leading the ACL from its low Last Interglacial to higher full glacial values (~ 30.4). The long-term increasing ACL trend is overprinted by rapid, millennial-scale, negative excursions (~ 0.3 – 0.4), mainly during the warm MIS 5c and 5a substages.

Branched glycerol dialkyl glycerol tetraethers (brGDGTs) concentrations vary between 0 and 250ng/g of dry sediment. Their variations in core GL-1090 follow the ACL pattern (Figure 2a), whereby lower concentrations are generally followed by reduced ACL, with the lowest values observed during MIS 5e. Rapid millennial-scale spikes lead brGDGT from its lower baseline to peaks of ~ 150 – 200 ng/g, mainly at the transition from late MIS 6 to 5e, during cold MIS 5 substages (MIS 5d and b), and at the end of MIS 5 (Figure 2b).

Discussion

Plant life form, function, and metabolic pathway have been found to dictate the chain length distribution of leaf waxes (ACL) in terrestrial plants[32–34]. Several studies have also provided evidence that climate factors (i.e., temperature and moisture) may modulate the ACL, consistent with the role of the leaf wax layer in regulating water loss of the plant. Positive (negative) relations between growth temperature (moisture availability) and *n*-alkane chain length (ACL) have been reported (e.g.,[35–40]). In our GL-1090 record, we can readily argue that temperature does not exert a dominant control on leaf wax chain length because higher ACL values are observed during cold glacial climates and not during warm intervals (Figure 2a).

The possible control of moisture on the ACL can be explored by considering long-term variations in rainfall patterns. In SE Brazil, rainfall is strongly controlled by the South American Summer Monsoon (SAMS)[41,42], the intensity of which is primarily driven by precession-forced changes in insolation[24,43]. Accordingly, high austral summer insolation during late MIS6 and Termination II would strengthen SAMS activity and rainfall in SE Brazil (Figure 3b), while the opposite would occur during MIS 5e (Figure 3b and c). Further, abrupt hydroclimate change occurred in the tropics during glacial Terminations, and a strengthening of SAMS rainfall[44–46] is largely reported, also linked to a southern placement of the Intertropical Convergence Zone (ITCZ) and decreased Atlantic cross-equatorial heat transport[47,48]. Data-model assessments indicate drier austral tropics during the Last Interglacial, with an accentuated decline of summer and spring and almost unchanged autumn/winter rainfall in South America[25]. Likewise, a speleothem $\delta^{18}O$ record from the Amazon region (and also under the influence of SAMS) shows a relatively weak monsoon during MIS 5e in phase with low austral summer insolation[49].

In core GL-1090, terrigenous inputs traced with soil-derived brGDGTs (Supplementary material; Supplementary Figure 1) are ultimately controlled by changes in the rainfall rate in SE Brazil. Their pattern indicates stronger runoff (intensified SAMS) during Termination II and lower rainfall (weakend SAMS) during the Last Interglacial (Fig 3d), supported by complementary multi-proxy magnetic and

isotopic studies[50,51]. Terrigenous supply from runoff is thus consistent with changes in rainfall rates dictated by austral summer insolation patterns (Figure 3b). The inferred decrease in monsoonal rainfall from the end of Termination II to MIS 5e is accompanied by a decrease in ACL values in core GL-1090 (Figure 3b), suggesting that a precipitation deficit is not pressuring plant life forms. This pattern strongly suggests that rainfall changes are unlikely the leading factor behind the observed ACL variation.

Having ruled out temperature and precipitation as the primary controls on ACL variations, we argue that the ACL record likely reflects vegetation changes in the adjacent hinterland. Among C_3 plants, deciduous and evergreen broadleaf trees (angiosperms) show overall lower ACL values (ca. ≤ 29-30) compared to herbaceous and conifer vegetation (ACL > 30), and C_3 savannah plants produce longer-chain *n*-alkanes (higher ACL) than the C_3 rainforest plants[33,52]. We thus propose that the ACL in core GL-1090 traces changes in the Atlantic Forest in SE Brazil with lower (higher) ACL indicating expansion (retraction) of the forest. A previous record in the study area has suggested using ACL as a proxy for changes in the Atlantic Forest[53]. In order to further constrain the ACL as a tracer of vegetation (Atlantic Forest) changes, we compared our results with available pollen data from the Colônia crater in SE Brazil located only a few kilometers from the shoreline[30]. The higher (~ 30.4) ACL values during late MIS 6 are consistent with the dominant presence of grassland vegetation composed of an association of *Poaceae*, conifers (*Araucaria* and *Podocarpus*), and shrubs[30] as the ones noted today at high elevation in the state of Paraná (southern Brazil)[54]. Toward the Last Interglacial, the vegetation composition fluctuated with the same species as during the penultimate glacial, except for the *Poaceae,* which decreased sharply, allowing shrubs to expand[55]. During MIS 5e, trees replaced shrubs, as shown in the high arboreal pollen frequencies[30], and this trend is mirrored in the concurrent smooth decreasing of ACL (Figures 3c and e).

Such a coherent variation between ACL and arboreal pollen data, already observed in other studies (e.g.[56]), strengthens our interpretation of ACL as a proxy of Atlantic Forest variations in SE Brazil. In this sense, the Last Interglacial likely shows the largest expansion of the arboreal cover of the Atlantic Forest over the studied period. Upon the demise of the Last Interglacial and towards MIS 4, a linear increasing trend is embedded in our ACL, with values reaching close to those of MIS 6 (Figure 3c). Throughout this interval, an orbital pattern is clearly distinguished following MIS 5 substages, with MIS 5d and b (MIS 5c and a) presenting a pattern toward higher (lower) ACL. Superimposed on this orbital scale, noticeable millennial-scale ACL negative excursions through MIS 5 substages likely indicate periods of short-term Atlantic Forest expansions briefly interrupting this long-term retraction.

Our data require a mechanism to account for the inferred variations of the Atlantic Forest vegetation distribution on orbital and millennial time scales. Here, we propose that these variations were primarily driven by the global atmospheric concentration of carbon dioxide, whereby elevated atmospheric CO_2 enhances forest plant growth through the “fertilization” effect (increased photosynthesis) and promotes decreased stomatal conductance that reduces transpiration (water loss)[8–10]. The role of this mechanism and its effect on biomass gains, biodiversity, and mortality rates, mainly over long-term periods, is still uncertain[57]. Modeling results with a potential vegetation model for Brazilian biomes indicated an

increase in humid forest cover for future high-emission scenarios, although this tends to be counteracted by decreasing precipitation and rising temperatures[57]. Based on our record and the complementary pollen data, we argue that raising atmospheric CO_2 during the penultimate deglaciation promoted the expansion of the Atlantic Forest in SE Brazil during MIS5e (Figure 3c). Interestingly, a similar conclusion is drawn by a pollen record combined with leaf wax data from the SE African margin. According to the authors, the development of interglacial woodlands would be primarily favored by higher CO_2 levels that allow decreased stomatal conductivity, relieving drought stress[17].

Aside from orbital variation, the ACL in core GL-1090 also varies on millennial time scales, revealing rapid changes in the SE Brazil biomes. During glacial intervals, the abrupt climate oscillations between the so-called Dansgaard-Oescheger (DO) stadial and interstadial conditions (Figures 3a and f) are linked with precipitation changes in (sub)tropical South America[24] that have the potential to promote a vegetation response. However, the wetter climate during Dansgaard-Oescheger (DO) stadials, shown in the Botuvera cave $\delta^{18}O$ record, does not involve lower ACL (i.e., forest expansion) (Figures 3a and c). In contrast, short-term forest expansion, denoted by lower ACL, is observed in DO interstadials (e.g., 19-21 and, to a lesser extent, 23-24 (Figures 3a and c)). The negative ACL excursions are nearly synchronous with millennial-scale CO_2 increments of ~10 – 20 ppm (Figures 3a and c), implying the role of CO_2 in driving a rapid Atlantic Forest response. Furthermore, the link between ACL (Atlantic Forest) and CO_2 is endorsed by the isospectral correlation, which yields a strong significant correlation between them ($R > -0.80$, $p < 0.01$) (Figure 3g).

Further, wavelet coherency analysis between ACL and CO_2 shows a well-defined anti-phased (180 º) signal taking place at precessional variability (~ 20 ka), which means that on orbital time scales, CO_2 and arboreal Atlantic Forest are synchronous. A wide coherency region at ~ 5 – 10 ka time scales could be related to large background changes of global atmospheric CO_2 since they occur at main transition periods (i.e., Termination II and MIS 5/4 boundary) (Figure 3g). The phase-angle during Termination II could still indicate a slight leading of atmospheric CO_2 related to the Atlantic Forest, which aligns with our interpretation.

Biome changes may impact the stability of the underlying soils as increasing vegetation cover (forest expansion) contributes to stabilizing and reducing soil erosion. The main peaks in soil material (brGDGT concentration) occur in periods of reduced arboreal cover (higher ACL) and enhanced precipitation (Figures 3a, c, and d), with this being conditioned by the core stratigraphy, disregarding chronological uncertainties (Figure 2). In this sense, our data highlight the dynamic response of the Atlantic rainforest and underlying soils in SE Brazil induced by global CO_2 changes.

Aiming to quantify the effects of CO_2 over biomass gains, we ran potential vegetation simulations with the CPTEC-PVM2 initialized with the 1961–1990 climatology[61], which reasonably reproduces the main South American biomes[29] (Figure 4). We evaluated the distribution of net primary productivity (kgC/m^2yr) in experiments where only CO_2 is changed from penultimate glacial (180 ppm) to Last

Interglacial (280 ppm) levels (Figure 4a). Simulations indicate that regions of tropical evergreen forest, which under the current climatology occur in the Amazon region and SE Brazil, suffer a loss in net primary productivity under penultimate glacial CO_2 concentration compared with the present (Figure 4b). Otherwise, when atmospheric CO_2 concentration is set to the Last Interglacial level, it favors a biomass gain of roughly 0.16 – 0.24 kgC/m²yr relative to glacial conditions (Figure 4b).

Future projections of vegetation cover in a range of conditions where only CO_2 or CO_2 and climate (temperature and precipitation) are considered suggest that tropical biomes are maintained or increase their productivity if the long-term CO_2 fertilization effect plays a role[29]. This positive feedback caused by atmospheric CO_2 is only countered if the dry season is longer than four months[29]. However, no observational evidence suggests that the CO_2 fertilization effect will likely play an important role in tropical forests on longer time scales[29]. In this sense, our data will work as long-term evidence that the CO_2 fertilization effect is a pervasive mechanism operating on millennial to orbital time scales. Evidently, the role of precipitation and temperature cannot be neglected[29]. Monitoring Brazilian non-Amazon tropical forests shows that recent drying and warming trends in the southeastern region have increased the annual carbon loss, turning carbon sink areas into carbon sources[62]. Considering this view, we hypothesize that past millennial-scale decreases in precipitation or even the drier condition of the Last Interglacial for the southern tropics[25] still yielded a sufficient rainfall supply to allow the CO_2 fertilization effect to occur. In this scenario, dry seasons likely do not exceed four months, and the range of CO_2 variability is not large enough to cause saturation within enzymatic scales[29]. Our study sheds light on the role of humid forests as carbon sinks during past periods of natural warming, working likely as negative feedback to slow down global warming and capture carbon released from the deep ocean. Deforestation of remaining Atlantic Forest areas seriously threatens any future carbon-induced biomass gain, urging protection and reforestation initiatives to preserve its natural long-term capacity in carbon storage.

Methods

Core GL-1090 and age model

Sediment core GL-1090 was collected in subtropical western South Atlantic (Santos basin - 24.92 ºS, 42.51 ºW) by Petrobras at a water depth of 2225 m. GL-1090 consists mostly of greenish to olive glacial sediments somewhat rich in foraminifera-bearing silty clay with Last Interglacial sediments represented by whitish clays[26]. The uppermost circulation in the region is dominated by the southward-flowing Brazil current that originates at ~ 10 ºS from the southern branch of the bifurcation of the South Equatorial Current[63]. Several minor rivers drain the narrow coastal plain north of the core location, with the Paraíba do Sul the most important. About 10 °S south of the GL-1090 site, the Plata River meets the subtropical Atlantic Ocean, in which the Plata Basin represents the largest source of terrigenous material to the western South Atlantic[50]. The chronology of the 1914 cm sediment length is resolved by radiocarbon dating and benthic foraminifera $\delta^{18}O$ tuning with sediment core MD95-2042. The age model employed

was modified after refs.[27,64] with a new tie-point collection during Termination II and throughout MIS 5. Final interpolation occurred on Bacon 2.3, which creates a more realistic Bayesian sediment accumulation history[65].

Average chain length of *n*-alkanes and brGDGT

The *n*-alkanes and brGDGTs were analyzed between 150.51 - 64.86 ka (689 – 1591 cm) along core GL-1090. Lipids were solvent extracted from freeze-dried sediments with sonication and separated into three fractions by silica gel chromatography following the procedures described in ref.[66]. *n*-alkanes were analyzed on an Agilent 6890N gas chromatography coupled to a flame ionization detector (GC-FID) and equipped with a 30 m DB-5 capillary column (0.32 mm internal diameter, 0.25 µm film thickness). The detector was set at 330 °C. The oven temperature program was initiated at 50 °C, increased by a rate of 30 °C min^{-1} to 120 °C, and subsequently by a rate of 5 °C min^{-1} until 320 °C (held for 10 min). Helium was used as carrier gas at constant flow (2.0 mL min^{-1}). The individual n-alkanes were quantified by comparing their peak area with the area of an internal standard. The average chain length (ACL; ref. [67]) was calculated using the most abundant C_{27} to C_{33} odd-carbon numbered n-alkanes; ACL= S ($i*X_i$)/ S X_i, where X is abundance, and i ranges from 27 to 33.

GDGTs (Glycerol dialkyl glycerol tetraethers) were analyzed by high-pressure liquid chromatography coupled with mass spectrometry with an atmospheric pressure chemical ionization source (HPLC–APCI-MS) using a Shimadzu LCMS 2020 in selected ion monitoring mode, equipped with two Acquity UHPLC BEH HILIC columns in tandem (150 mm × 2.1 mm, 1.7 µm; Waters, USA), thermally controlled at 40 ◦C; following the procedure detailed in ref. [68].

Potential Vegetation Model

We used the Center for Weather Forecasting and Climate Studies Potential Vegetation Model version 2 (CPTEC-PVM2). This model is skillful in reproducing the main South American biomes like tropical forests over Amazonia and the Atlantic coastal region, savannas over central Brazil (‘cerrado’), dry shrublands (‘caatinga’) over northeastern Brazil and the Chaco region, grasslands over the Pampas, and semidesert vegetation over Patagonia[57,29]. CPTEC-PVM2 shows a reasonable performance over South America due to considering seasonality as a factor delimitating savannas and forests. CPTEC-PVM2 takes into account plant physiological responses to this seasonality. The biome allocation rules rely mainly on a given grid cell's optimum net primary productivity values, which demands gross primary productivity and plant respiration calculation. This is done aside with a water balance submodel using 1961 – 1990 surface temperature and precipitation climatologies from http://climate.geog.udel.edu/~climate/html_pages/download.html. Global and especially South American net primary productivity simulated by CPTEC-PVM2 is comparable to that from observations and other models[29]. In this study, we run a “CO_2-only” experiment with atmospheric carbon dioxide concentrations relative to the penultimate glacial maximum (180 ppm) and Last Interglacial (280 ppm) in

which the climate (precipitation and temperature) are kept unchanged as taken from 1961 – 1990 average.

Correlation analysis

Correlation exercises were done in the Python 3.9 application Pyleoclim[69]. Merged atmospheric CO_2 from refs.[22,23] and GL-1090 ACL were previously interpolated to their mean resolution and standardized with respective Pyleoclim tools. We used time-series correlation with the default isospectral method accompanied by 5,000 Monte Carlo runs. Wavelet coherence analysis was realized over the same data pair with 1,000 Monte Carlo runs.

Declarations

Acknowledgments

We acknowledge Petrobras by the cession of sediment core GL-1090. This work was supported by the BARISTA project funded through the French National program LEFE, and by the CAPES/Paleoceano Project (23038.001417/2014e7), CAPES-IODP/Aspecto Project (88887.091731/2014e01), Project CLIMATE/Print-CAPES (88887.310301/2018e00). We acknowledge the support of the CAPES-COFECUB program through their funding of actions 32/2022 and Te 1003/23 (project numbers 8881.712022/2022-1 and 49558SM) and by the CNRS-France International Research Project SARAVA (Drivers of past changes in South Atlantic circulation and tropical South American climate). TPS also thanks the Programa de Apoio a Novos Docentes (process 22.1.09345.01.2) of the University of São Paulo. JFC thanks the support provided by CNPq (140443/2016e9) and CAPES/Programas Estrategicos (88881.145911/2017e01). RAN thanks the French Ministry of Europe and Foreign Affairs for its financial support within the MOPGA Fellowship Program. IMV acknowledges the support of FAPERJ (SEI-260003/000677/2023) (JCNE grant 200.120/2023–281226)

Author contribution

TPS: Writing - Original Draft, Conceptualization, Formal analysis, Data Curation. IB: Writing - Original Draft, Writing - Review & Editing, Resources, Supervision, Funding acquisition. JFC: Formal analysis, Investigation. AMSR: Formal analysis, Investigation. MPL: Writing - Review & Editing, Data Curation. AH: Writing - Review & Editing, Resources, Supervision, Funding acquisition. MHS: Formal analysis. MRL: Formal analysis. RAN: Writing - Review & Editing. IMV: Writing - Review & Editing. RLS: Writing - Review & Editing, Formal analysis. MCB: Writing - Review & Editing, Formal analysis, Supervision. ALSA: Supervision, Project administration, Funding acquisition.

Data availability statement

Data generated for this study accompanies the submission as supplementary material.

Competing Interests Statement

Authors declare non-financial competing interests

References

1. Myers, N., Mittermeier, R. A., Mittermeier, C. G., Da Fonseca, G. A. B. & Kent, J. Biodiversity hotspots for conservation priorities. *Nature* **403**, 853–858 (2000).
2. Ribeiro, M. C. *et al.* The Brazilian Atlantic Forest: A Shrinking Biodiversity Hotspot. in *Biodiversity Hotspots* (eds. Zachos, F. E. & Habel, J. C.) 405–434 (Springer Berlin Heidelberg, Berlin, Heidelberg, 2011). doi:10.1007/978-3-642-20992-5_21.
3. Ferretti, A. R. & De Britez, R. M. Ecological restoration, carbon sequestration and biodiversity conservation: The experience of the Society for Wildlife Research and Environmental Education (SPVS) in the Atlantic Rain Forest of Southern Brazil. *Journal for Nature Conservation* **14**, 249–259 (2006).
4. Mittermeier, R. A., Turner, W. R., Larsen, F. W., Brooks, T. M. & Gascon, C. Global Biodiversity Conservation: The Critical Role of Hotspots. in *Biodiversity Hotspots* (eds. Zachos, F. E. & Habel, J. C.) 3–22 (Springer Berlin Heidelberg, Berlin, Heidelberg, 2011). doi:10.1007/978-3-642-20992-5_1.
5. Borma, L. S. *et al.* Beyond Carbon: The Contributions of South American Tropical Humid and Subhumid Forests to Ecosystem Services. *Reviews of Geophysics* **60**, e2021RG000766 (2022).
6. Le Quéré, C. *et al.* Global Carbon Budget 2017. *Earth Syst. Sci. Data* **10**, 405–448 (2018).
7. Chen, C., Riley, W. J., Prentice, I. C. & Keenan, T. F. CO_2 fertilization of terrestrial photosynthesis inferred from site to global scales. *Proc. Natl. Acad. Sci. U.S.A.* **119**, e2115627119 (2022).
8. Kattge, J., Knorr, W., Raddatz, T. & Wirth, C. Quantifying photosynthetic capacity and its relationship to leaf nitrogen content for global-scale terrestrial biosphere models. *Global Change Biology* **15**, 976–991 (2009).
9. Janssens, I. A. *et al.* Reduction of forest soil respiration in response to nitrogen deposition. *Nature Geosci* **3**, 315–322 (2010).
10. Peng, J., Dan, L. & Dong, W. Are there interactive effects of physiological and radiative forcing produced by increased CO2 concentration on changes of land hydrological cycle? *Global and Planetary Change* **112**, 64–78 (2014).
11. Schimel, D., Stephens, B. B. & Fisher, J. B. Effect of increasing CO_2 on the terrestrial carbon cycle. *Proc. Natl. Acad. Sci. U.S.A.* **112**, 436–441 (2015).
12. Huntingford, C. *et al.* Simulated resilience of tropical rainforests to CO2-induced climate change. *Nature Geosci* **6**, 268–273 (2013).
13. Clark, D. A., Piper, S. C., Keeling, C. D. & Clark, D. B. Tropical rain forest tree growth and atmospheric carbon dynamics linked to interannual temperature variation during 1984–2000. *Proc. Natl. Acad. Sci. U.S.A.* **100**, 5852–5857 (2003).
14. Wang, S. *et al.* Recent global decline of CO_2 fertilization effects on vegetation photosynthesis. *Science* **370**, 1295–1300 (2020).

15. Reichgelt, T. *et al. Elevated CO₂, Increased Leaf-Level Productivity and Water-Use Efficiency during the Early Miocene*. https://cp.copernicus.org/preprints/cp-2020-30/cp-2020-30.pdf (2020) doi:10.5194/cp-2020-30.
16. Yang, J.-W. *et al.* Global biosphere primary productivity changes during the past eight glacial cycles. *Science* **375**, 1145–1151 (2022).
17. Dupont, L. M., Caley, T. & Castañeda, I. S. Effects of atmospheric CO₂ variability of the past 800 kyr on the biomes of southeast Africa. *Clim. Past* **15**, 1083–1097 (2019).
18. O'Mara, N. A. *et al.* Pleistocene drivers of Northwest African hydroclimate and vegetation. *Nat Commun* **13**, 3552 (2022).
19. Behling, H. Carbon storage increases by major forest ecosystems in tropical South America since the Last Glacial Maximum and the early Holocene. *Global and Planetary Change* **33**, 107–116 (2002).
20. Buso Junior, A. A. *et al.* Late Pleistocene and Holocene Vegetation, Climate Dynamics, and Amazonian Taxa in the Atlantic Forest, Linhares, SE Brazil. *Radiocarbon* **55**, 1747–1762 (2013).
21. Francisquini, M. I. *et al.* Cold and humid Atlantic Rainforest during the last glacial maximum, northern Espírito Santo state, southeastern Brazil. *Quaternary Science Reviews* **244**, 106489 (2020).
22. Bereiter, B. *et al.* Mode change of millennial CO2 variability during the last glacial cycle associated with a bipolar marine carbon seesaw. *Proceedings of the National Academy of Sciences* **109**, 9755–9760 (2012).
23. Lüthi, D. *et al.* High-resolution carbon dioxide concentration record 650,000–800,000 years before present. *Nature* **453**, 379–382 (2008).
24. Cruz, F. W. *et al.* Insolation-driven changes in atmospheric circulation over the past 116,000 years in subtropical Brazil. *Nature* **434**, 63–66 (2005).
25. Scussolini, P. *et al.* Agreement between reconstructed and modeled boreal precipitation of the Last Interglacial. *Sci. Adv.* **5**, eaax7047 (2019).
26. Santos, T. P. *et al.* Prolonged warming of the Brazil Current precedes deglaciations. *Earth and Planetary Science Letters* **463**, 1–12 (2017).
27. Santos, T. P. *et al.* Asymmetric response of the subtropical western South Atlantic thermocline to the Dansgaard-Oeschger events of Marine Isotope Stages 5 and 3. *Quaternary Science Reviews* **237**, 106307 (2020).
28. Ledru, M., Montade, V., Blanchard, G. & Hély, C. Long-term Spatial Changes in the Distribution of the Brazilian Atlantic Forest. *Biotropica* **48**, 159–169 (2016).
29. Lapola, D. M., Oyama, M. D. & Nobre, C. A. Exploring the range of climate biome projections for tropical South America: The role of CO_2 fertilization and seasonality: FUTURE BIOME DISTRIBUTION IN SOUTH AMERICA. *Global Biogeochem. Cycles* **23**, n/a-n/a (2009).
30. Ledru, M. P., Mourguiart, P. & Riccomini, C. Related changes in biodiversity, insolation and climate in the Atlantic rainforest since the last interglacial. *Palaeogeography, Palaeoclimatology,*

Palaeoecology **271**, 140–152 (2009).

31. Tian, D. *et al.* PyGMT: A Python interface for the Generic Mapping Tools. Zenodo https://doi.org/10.5281/ZENODO.3781524 (2023).
32. Eglinton, G. & Hamilton, R. J. Leaf Epicuticular Waxes: The waxy outer surfaces of most plants display a wide diversity of fine structure and chemical constituents. *Science* **156**, 1322–1335 (1967).
33. Bush, R. T. & McInerney, F. A. Leaf wax n-alkane distributions in and across modern plants: Implications for paleoecology and chemotaxonomy. *Geochimica et Cosmochimica Acta* **117**, 161–179 (2013).
34. Eglinton, T. I. & Eglinton, G. Molecular proxies for paleoclimatology. *Earth and Planetary Science Letters* **275**, 1–16 (2008).
35. Bush, R. T. & McInerney, F. A. Influence of temperature and C 4 abundance on n -alkane chain length distributions across the central USA. *Organic Geochemistry* **79**, 65–73 (2015).
36. Castañeda, I. S., Werne, J. P., Johnson, T. C. & Filley, T. R. Late Quaternary vegetation history of southeast Africa: The molecular isotopic record from Lake Malawi. *Palaeogeography, Palaeoclimatology, Palaeoecology* **275**, 100–112 (2009).
37. Schefuß, E., Ratmeyer, V., Stuut, J.-B. W., Jansen, J. H. F. & Sinninghe Damsté, J. S. Carbon isotope analyses of n-alkanes in dust from the lower atmosphere over the central eastern Atlantic. *Geochimica et Cosmochimica Acta* **67**, 1757–1767 (2003).
38. Vogts, A., Schefuß, E., Badewien, T. & Rullkötter, J. n-Alkane parameters from a deep sea sediment transect off southwest Africa reflect continental vegetation and climate conditions. *Organic Geochemistry* **47**, 109–119 (2012).
39. Horikawa, K., Murayama, M., Minagawa, M., Kato, Y. & Sagawa, T. Latitudinal and Downcore (0–750 ka) Changes in Nalkane Chain Lengths in the Eastern Equatorial Pacific. *Quat. res.* **73**, 573–582 (2010).
40. Rommerskirchen, F. *et al.* A north to south transect of Holocene southeast Atlantic continental margin sediments: Relationship between aerosol transport and compound-specific δ^{13} C land plant biomarker and pollen records. *Geochem Geophys Geosyst* **4**, 2003GC000541 (2003).
41. Garreaud, R. D., Vuille, M., Compagnucci, R. & Marengo, J. Present-day South American climate. *Palaeogeography, Palaeoclimatology, Palaeoecology* **281**, 180–195 (2009).
42. Vuille, M. *et al.* A review of the South American monsoon history as recorded in stable isotopic proxies over the past two millennia. *Clim. Past* **8**, 1309–1321 (2012).
43. Mohtadi, M., Prange, M. & Steinke, S. Palaeoclimatic insights into forcing and response of monsoon rainfall. *Nature* **533**, 191–199 (2016).
44. Stríkis, N. M. *et al.* South American monsoon response to iceberg discharge in the North Atlantic. *Proceedings of the National Academy of Sciences of the United States of America* 201717784 (2018) doi:10.1073/pnas.1717784115.

45. Novello, V. F. *et al.* A high-resolution history of the South American Monsoon from Last Glacial Maximum to the Holocene. *Scientific Reports* **7**, 44267 (2017).
46. Stríkis, N. M. *et al.* Timing and structure of Mega-SACZ events during Heinrich Stadial 1. *Geophysical Research Letters* 1–8 (2015) doi:10.1002/2015GL064048.Received.
47. Chiang, J. C. H., Cheng, W. & Bitz, C. M. Fast teleconnections to the tropical Atlantic sector from Atlantic thermohaline adjustment. *Geophysical Research Letters* **35**, 1–5 (2008).
48. McGee, D., Donohoe, A., Marshall, J. & Ferreira, D. Changes in ITCZ location and cross-equatorial heat transport at the Last Glacial Maximum, Heinrich Stadial 1, and the mid-Holocene. *Earth and Planetary Science Letters* **390**, 69–79 (2014).
49. Cheng, H. *et al.* Climate change patterns in Amazonia and biodiversity. *Nat Commun* **4**, 1411 (2013).
50. Mathias, G. L. *et al.* A Multi-Proxy Approach to Unravel Late Pleistocene Sediment Flux and Bottom Water Conditions in the Western South Atlantic Ocean. *Paleoceanography and Paleoclimatology* **36**, 1–22 (2021).
51. Figueiredo, T. S., Bergquist, B. A., Santos, T. P., Albuquerque, A. L. S. & Silva-Filho, E. V. Relationship between glacial CO2 drawdown and mercury cycling in the western South Atlantic: An isotopic insight. *Geology* (2022) doi:10.1130/g49942.1.
52. Diefendorf, A. F. & Freimuth, E. J. Extracting the most from terrestrial plant-derived n-alkyl lipids and their carbon isotopes from the sedimentary record: A review. *Organic Geochemistry* **103**, 1–21 (2017).
53. Dauner, A. L. L. *et al.* Late Pleistocene to Holocene variations in marine productivity and terrestrial material delivery to the western South Atlantic. *Front. Mar. Sci.* **9**, 924556 (2022).
54. Scheer, M. B., Curcio, G. R. & Roderjan, C. V. Carbon and Water in Upper Montane Soils and Their Influences on Vegetation in Southern Brazil. *ISRN Soil Science* **2013**, 1–12 (2013).
55. Aviles, A. M. C., Ledru, M., Ricardi-Branco, F., Marquardt, G. C. & De Campos Bicudo, D. The southern Brazilian tropical forest during the penultimate Pleistocene glaciation and its termination. *J Quaternary Science* jqs.3594 (2024) doi:10.1002/jqs.3594.
56. Badewien, T., Vogts, A., Dupont, L. & Rullkötter, J. Influence of Late Pleistocene and Holocene climate on vegetation distributions in southwest Africa elucidated from sedimentary n-alkanes – Differences between 12°S and 20°S. *Quaternary Science Reviews* **125**, 160–171 (2015).
57. Maksic, J. *et al.* Brazilian biomes distribution: Past and future. *Palaeogeography, Palaeoclimatology, Palaeoecology* **585**, 110717 (2022).
58. Bazin, L. *et al.* An optimized multi-proxy, multi-site Antarctic ice and gas orbital chronology (AICC2012): 120-800 ka. *Climate of the Past* **9**, 1715–1731 (2013).
59. Veres, D. *et al.* The Antarctic ice core chronology (AICC2012): An optimized multi-parameter and multi-site dating approach for the last 120 thousand years. *Climate of the Past* **9**, 1733–1748 (2013).

60. Laskar, J. *et al.* A long-term numerical solution for the insolation quantities of the Earth. *Astronomy & Astrophysics* **428**, 261–285 (2004).
61. Willmott, C.J. & Matsuura, K. Terrestrial Air Temperature and Precipitation: Monthly and Annual Time Series (1950–1999) Version 1.02.
62. Maia, V. A. *et al.* The carbon sink of tropical seasonal forests in southeastern Brazil can be under threat. *Sci. Adv.* **6**, eabd4548 (2020).
63. Stramma, L. & England, M. On the water masses and mean circulation of the South Atlantic Ocean. *Journal of Geophysical Research: Oceans* **104**, 20863–20883 (1999).
64. Ballalai, J. M. *et al.* Tracking Spread of the Agulhas Leakage Into the Western South Atlantic and Its Northward Transmission During the Last Interglacial. *Paleoceanography and Paleoclimatology* **34**, 1744–1760 (2019).
65. Blaauw, M., Christen, J. A., Bennett, K. D. & Reimer, P. J. Double the dates and go for Bayes — Impacts of model choice, dating density and quality on chronologies. *Quaternary Science Reviews* **188**, 58–66 (2018).
66. Cruz, J. F. *et al.* Multiproxy reconstruction of late quaternary upper ocean temperature in the subtropical southwestern Atlantic. *Quaternary Science Reviews* **307**, 108044 (2023).
67. *Proceedings of the Ocean Drilling Program, 116 Scientific Results*. vol. 116 (Ocean Drilling Program, 1990).
68. Rouyer-Denimal, L. *et al.* Subsurface warming in the tropical Atlantic for the last 3 deglaciations: Insights from organic molecular proxies. *Quaternary Science Reviews* **321**, 108370 (2023).
69. Khider, D. *et al.* Pyleoclim: Paleoclimate Timeseries Analysis and Visualization With Python. *Paleoceanog and Paleoclimatol* **37**, (2022).

Figures

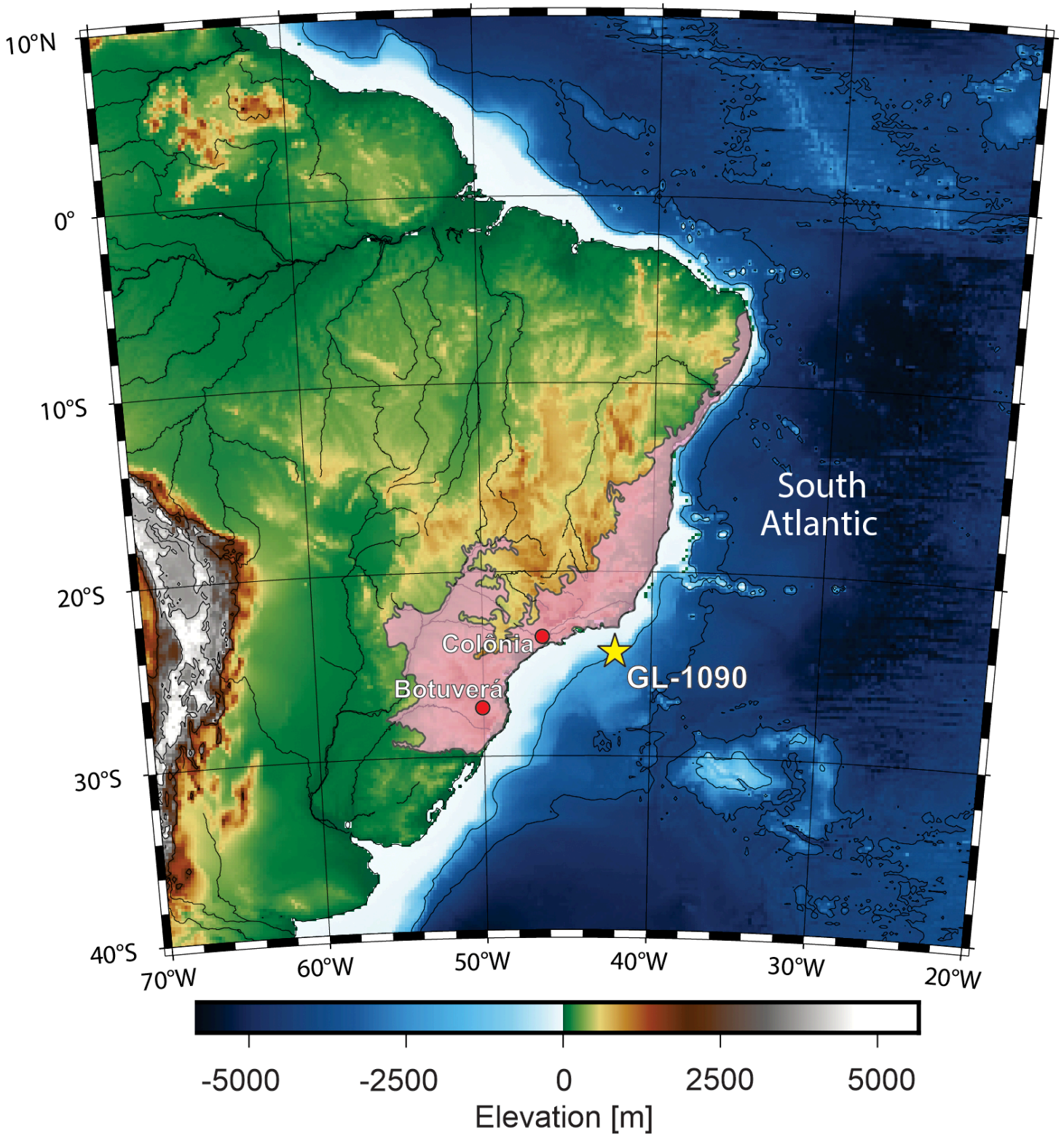

Figure 1

Position of sediment core GL-1090 (yellow star – this study) in the western South Atlantic (Santos basin) and other continental records discussed (red circles - Colônia crater[30] and Botuverá cave[24]). The pink highlighted area presents the original cover of the Atlantic Forest in eastern South America. This figure has been partially done with PyGMT[31].

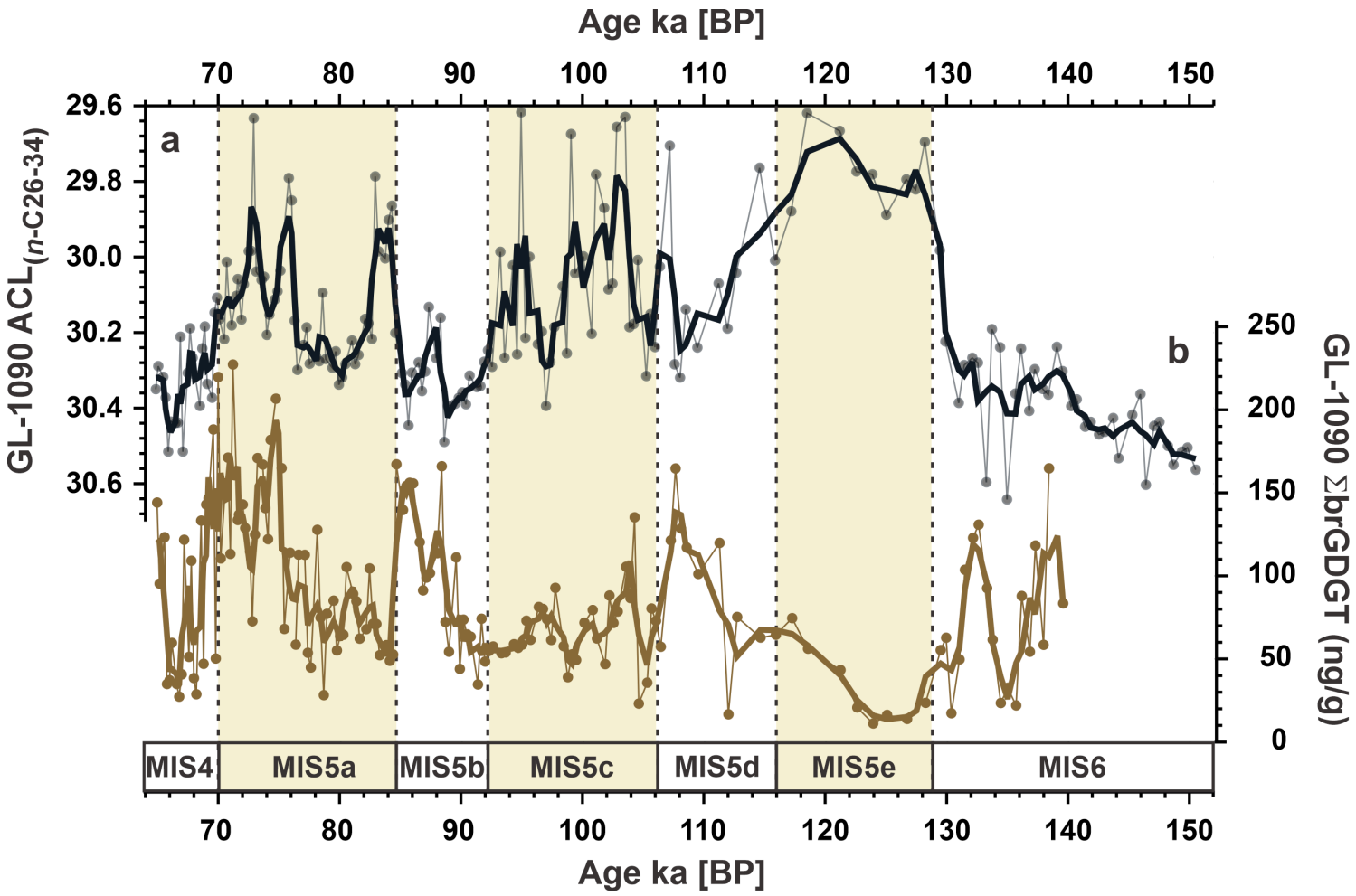

Figure 2

Results of core GL-1090 average chain length (ACL) of n-alkanes and branched glycerol dialkyl glycerol tetraethers (brGDGTs) concentrations from Marine Isotope Stage (MIS) 6 to 4. (a) GL-1090 ACL (thin black line and dots) with 3-points moving average (thick black line). (b) GL-1090 brGDGT (brown line and dots) with 3-point moving average (thick brown line). Vertical yellow bars denote the Last Interglacial and warm MIS 5 substages.

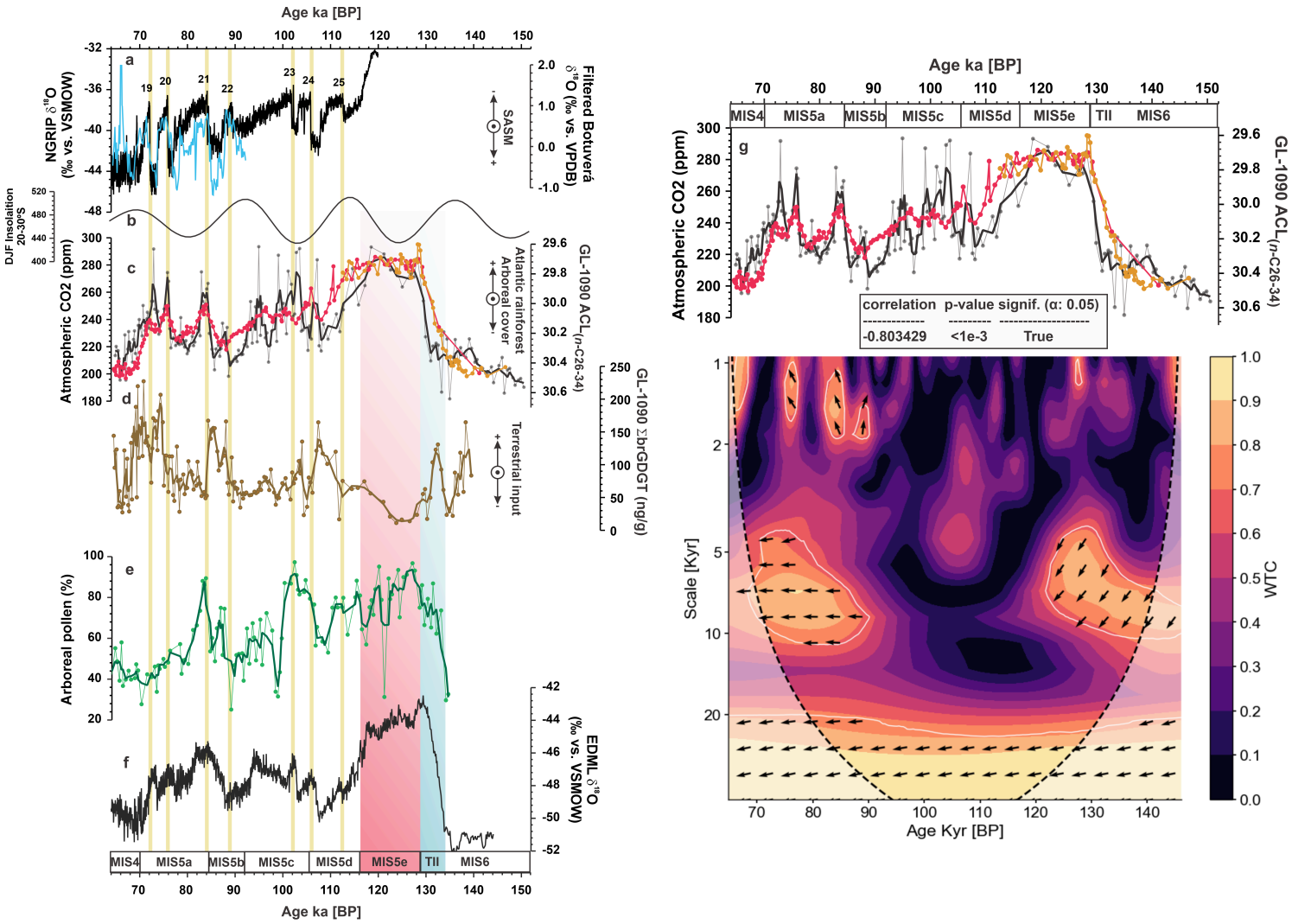

Figure 3

Results of core GL-1090 average chain length (ACL) and branched glycerol dialkyl glycerol tetraether (brGDGT) concentrations in the context of Marine Isotope Stage (MIS) 6 to 4. (a) NGRIP $\delta^{18}O$ at the AICC2012 time scale[58,59] (black) and high band-pass filtering of the Boutuverá cave $\delta^{18}O$[24] (blue). (b) austral summer insolation between 20 – 30 ºS[60]. (c) GL-1090 ACL (thin black line and dots) with 3-point moving average (thick black line) and atmospheric CO_2 from Antarctica ice cores from refs.[23] (orange) and ref. [22] (red). (d) GL-1090 brGDGT (brown, black line and dots) with 3-point moving average (thick brown line). (e) Colônia crater arboreal pollen data from ref.[30]. (f) EDML $\delta^{18}O$ at the AICC2012 time scale[58,59]. (g) GL-1090 ACL and atmospheric CO_2 with the isospectral correlation and wavelet transform coherency.

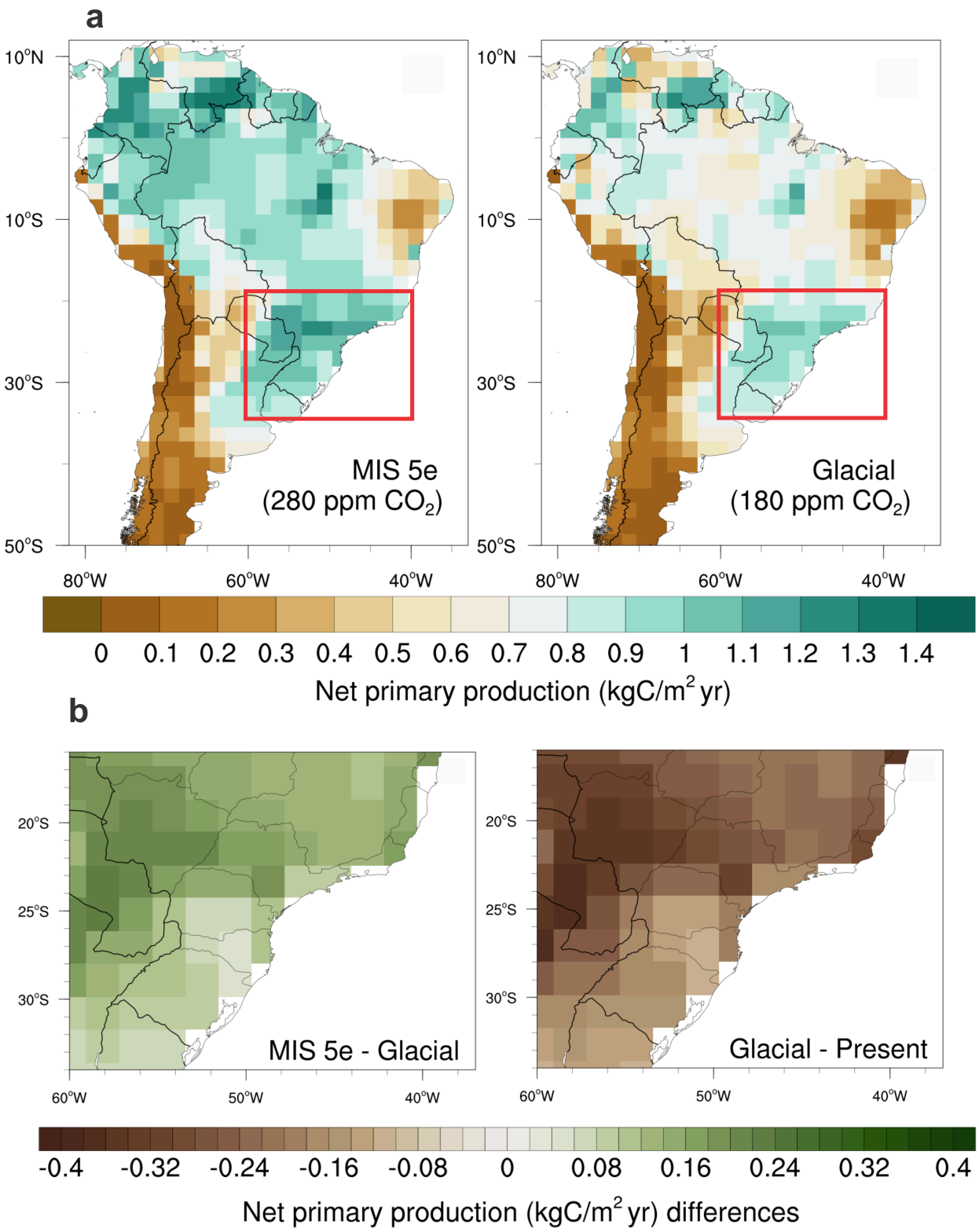

Figure 4

"CO_2-only" experiment conducted with Center for Weather Forecasting and Climate Studies Potential Vegetation Model version 2 (CPTEC-PVM2) in which precipitation and temperature are kept unchanged referent to 1961 – 1990 mean climatology. (a) Net primary productivity under the Last Interglacial (left) and penultimate glacial maximum (right) CO_2 concentrations. (b) Net primary productivity difference

between Last Interglacial and penultimate glacial (left) and penultimate glacial and mean 1961 – 1990 CO_2 concentration (right).

Supplementary Files

This is a list of supplementary files associated with this preprint. Click to download.

- GL1090data.csv
- Supplementarymaterial.docx
- Supplementaryfigure1.tif